DOI 10.4430/bgo00433

Geomagnetic signature of the Sabzevar ophiolite belt in north-eastern Iran

S.H. Hosseini[1], S.M. Ghiasi[1], S. Ghanbarifar[1], M. Abedi[2] and A. Afshar[3]

[1] *Institute of Geophysics, University of Tehran, Tehran, Iran*
[2] *School of Mining Engineering, College of Engineering, University of Tehran, Tehran, Iran*
[3] *Department of Mining and Metallurgical Engineering, Amirkabir University of Technology, Tehran, Iran*

(Received: 12 February 2023; accepted: 12 August 2023; published online: 25 October 2023)

ABSTRACT Ophiolite zones in Iran are capable of bearing precious minerals, which indicates the importance of undertaking investigations into ophiolite belts. Although the north-eastern ophiolites of Iran cover a vast area, they should be better recognised in terms of geophysical features and properties. The Sabzevar ophiolite area is an orogenic and subducted zone with typical ophiolite series, including sedimentary, crustal and mantle sequences. This study sets out to characterise the auspicious igneous and ophiolite zones in the frame of large-scale and tectonic conditions, geometrical shapes, expansions, and deep susceptibility features through novel magnetic synthesis interpretation techniques. In order to study the mentioned area, airborne magnetometry data over 60,000 km^2 have been utilised. Thus, geophysical research has been conducted to define the tectonic and ophiolite zones of the Sabzevar area by means of magnetic methods including edge detection techniques and 3D susceptibility models. In this research, newly developed edge-detection filters of *MNTHD* and *MNTDR* are applied to the aeromagnetic data to identify the shape and boundary of the anomalies at the Sabzevar ophiolite. In addition, edge detection would facilitate dividing the study area into smaller sectors, as proper targets, for running 3D inversion schemes precisely. This study uses qualitative analysis to gain insights into the subsurface structure status. The simultaneous interpretation of edge detection results and 3D inverted models would lead the way to dependable outcomes. The study area consists of six ophiolite sections, pre-identified by geological and geochemical approaches. These are the basis for this research which primarily studies the Sabzevar ophiolitic area. In order to conduct a detailed investigation into the study area, seven blocks were considered for the inverse modelling procedure. Consequently, the 3D susceptibility models matched the edge detection results accurately. Finally, as a multidisciplinary geophysical investigation over a large-scale ophiolite belt, the inverted susceptibility models of the whole area were overlaid with the geological and magnetic edge detection maps, unifying a solid view of the deep underground structures.

Key words: Sabzevar ophiolite, *MNTHD* and *MNTDR* filters, 3D inverse modelling, synthesis interpretation.

1. Introduction

Ophiolites were introduced for the first time by Brongniart (1821). Keeping information from ocean basin annals and progression, ophiolites provide critical details on the chemical and physical properties of the mantle. Forming within the orogenic zones, ophiolites can be

treasured targets for geophysical surveys due to the existence of natural elements, such as gold, silver, platinum, ferrous metals, and chromium, in the ultramafic rocks (Dilek and Furnes, 2014; Michels *et al*., 2018). The Sabzevar-Torbat-e-Heydarieh ophiolite belt, also called the Sabzevar ophiolite, is a vast sequence of occurrences along the northern border of continental crust of the central Iranian zone. Generally, ophiolites are a complex of peridotite, gabbro, dibasic, basaltic, and soft oceanic alluvial layers, which can be extensively found in subduction and collision zones. Hence, ophiolites belong to the Earth's oceanic crust or upper mantle, which has been raised and exposed above the sea level. This type of large-scale structural formation is among the main geological factors providing mineral exploratory opportunities. Ophiolites principally emerge along suture areas and play a significant role in the recognition of ancient oceanic lithosphere and paleogeographic reconstructions of orogenic belts (Coleman, 1977; Dilek, 2003; Dilek and Furnes, 2011). Within most ophiolite areas in Iran, the sequences are disordered, and known as ophiolite *mélange*. As mentioned, ophiolite zones are essentially due to their metal and non-metal mineral resources, especially chromium and manganese. In this research, in order to characterise and properly locate the ophiolite zones and borders, airborne magnetic data were utilised. There are numerous advantages of airborne geophysical techniques, including covering a large area quickly and effectively, performing survey operations in areas inaccessible by ground surveys, providing equidistant data and helping in efficient interpretations of tectonic purposes, determining exploratory targets for conducting complementary ground studies, and obtaining geological, structural, and regional information (Gandhi and Sarkar, 2016). Therefore, airborne magnetic surveying can be very prompt and appropriate for detecting large-scale subsurface anomalies with no outcrops.

The aeromagnetic data used in this research were obtained between 1974 and 1978, with 7.5 km of flight spacing at 500-2000 m of altitude, depending on the topography. It is important to underline that this survey covers most of the study area except for some partial zones (Yousefi and Feriedberg, 1977; Ghobadian *et al*., 2014). First, the acclaimed reduction to the pole filter has been used to process magnetic grids (Nabighian, 1972, 1974). In magnetometry studies, the Reduction to the Pole (RTP) filter is a frequent tool, which facilitates interpreting multi-source anomalies. It converts magnetic signals to symmetrical patterns, i.e. magnetic data are only induced with the vertical component of the Earth's magnetic field. The RTP map actually eliminates the dipolar nature of magnetic anomalies by shifting anomaly peaks over the main causative sources (Abedi and Oskooi, 2015; Hosseini *et al*., 2021). Here following, newly developed Modified-Normalised Total Horizontal Derivative (*MNTHD*) and Modified-Normalised Tilt Derivative (*MNTDR*) edge detection filters have been applied on the aeromagnetic grids to accurately indicate the anomaly boundaries (Ghiasi *et al*., 2023). Edge detection methods are practicable approaches for processing and interpreting potential field data used to distinguish the subsurface anomaly properties in shape and position (Blakely, 1996). Therefore, it seems that using edge detection would help to determine the main structures in the study area. The *MNTHD* filter is expected to detect smoother edges with high resolution and illustrate narrower edges with extra details, but, as a result of its formula, some minor false edges and noises may be more evident. Next, a 3D inverse modelling was run through the aeromagnetic data to investigate the susceptibility features of both surface and underground structures (Li and Oldenburg, 1996, 1998). It is believed that simultaneous and synthesis interpretation of the study area, in terms of edge detection and 3D inverse modelling, may be instrumental in more accurately and comprehensively characterising the Sabzevar ophiolite zones. Ultimately, the thorough conceptual model of the highly susceptible model, overlaid by geological maps, edge detection results and magnetic maps, would be applicable for acquiring knowledge of the

area for additional complementary studies. Combining the improved edge-detection techniques mentioned with the 3D inverse modelling scheme, Ghiasi *et al*. (2023) presented a novel approach to achieve proper edge polygons superimposed on the high susceptibility zone on which drilling spots could be easily located. In this research, the above-mentioned approach is utilised over a large-scale ophiolite case to obtain a reliable edge perimeter along with multiple 3D models as a means for further geophysical exploratory investigations.

Fig. 1 illustrates the geological map of Iran by highlighting the main ophiolite belts. As shown, the study area, consisting of the Sabzevar-Torbat-e-Heydarieh ophiolite belt, is indicated in blue dashed boxes. The study area, over 350 km long (E-W), is also surrounded by the Binalud Mountains (Kopeh Daq) to the north and by the sizable Dorouneh sinistral strike-slip fault to the south, separating the area from the Lut Block (Nozaem *et al*., 2013). The Sabzevar ophiolite area has been studied in terms of tectonic properties as well (formerly by Baroz *et al*., 1983, 1984; Desmons and Beccaluva, 1983; Ohnenstetter and Sider, 1988; Shojaat *et al*., 2003; Rossetti *et al*., 2010; Omrani *et al*., 2013).

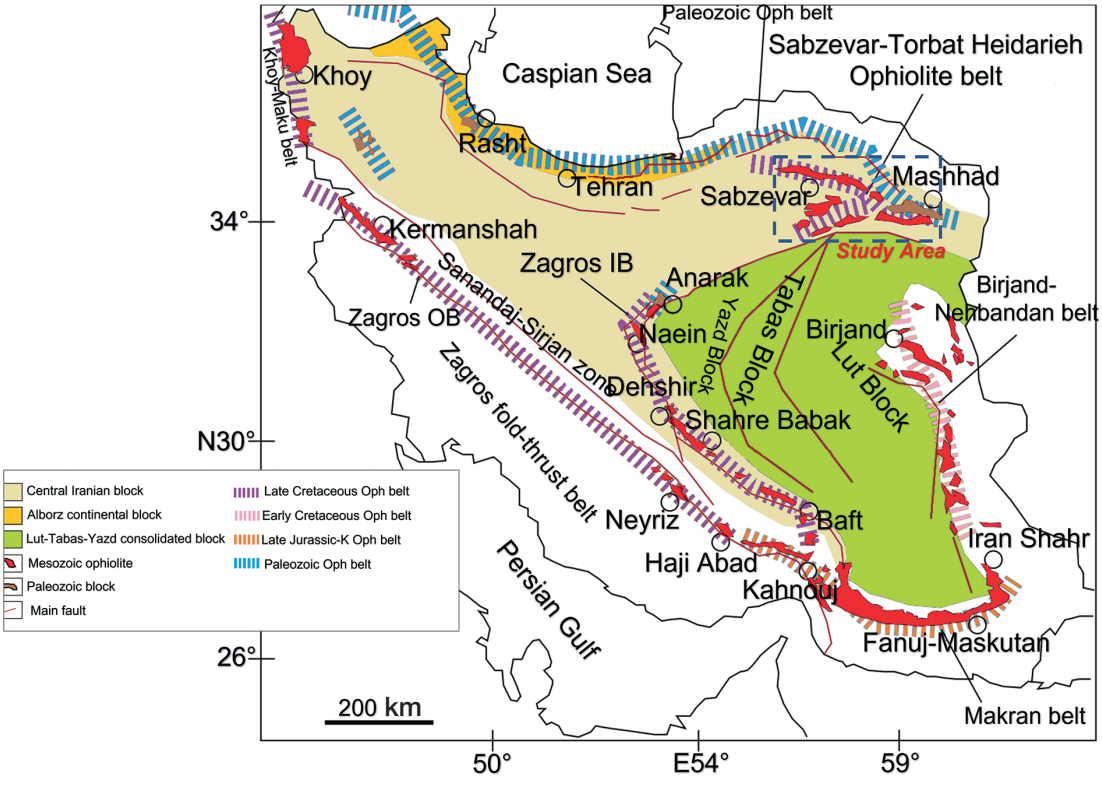

Fig. 1 - Main ophiolite belts superimposed over the simplified geological map of Iran (Moghadam *et al*., 2014).

2. Edge detection techniques

This study utilised the Ghiasi *et al*. (2023) approaches to accurately obtain the edges of the magnetic anomalies. As summarily stated, the *MNTHD* filter simultaneously uses horizontal (*THD*) and vertical (d^2f/dz^2) derivatives of potential field data, which would reduce the false edges and enhance the resolution of the edge perimeters.

The *MNTHD* equation is as follows:

$$MNTHD = \tan^{-1}\left\{\frac{THD \times \frac{min(\partial^2 f/\partial z^2)}{max(\partial^3 f/\partial z^3)}}{|\partial^2 f/\partial z^2| + p \times max\left[THD \times \frac{min(\partial^2 f/\partial z^2)}{max(\partial^3 f/\partial z^3)}\right]}\right\} \quad (1)$$

where *f* is the total potential field data, *THD* is the Total Horizontal Derivative (Cordell and Grauch, 1985), and *p* is an adjustment parameter between 0 and 0.5. The maximum *MNTHD* values indicate the edges of the potential anomalies filed.

The *MNTDR* edge detection filter (Ghiasi *et al*., 2023), an improved version of the *THDR* filter (Verduzco *et al*., 2004), utilises multiple horizontal and vertical derivatives in its formula. The *MNTDR* filter, therefore, shows narrower edges and more details, yet it can sometimes be more contaminated by noise and false edges than the *MNTHD*. The *MNTDR* equation is written as:

$$MNTDR = \tan^{-1}\left\{\frac{THDR \times \frac{min(\partial^2 f/\partial z^2)}{max(\partial^3 f/\partial z^3)}}{|\partial^2 f/\partial z^2| + p \times max\left[THDR \times \frac{min(\partial^2 f/\partial z^2)}{max(\partial^3 f/\partial z^3)}\right]}\right\} \quad (2)$$

where *f* is the total potential field data, *THDR* is the *THDs* of the tilt angle filter (Miller and Singh, 1994), and *p* is an adjustment parameter between 0 and 0.5, which should be determined by the interpreter. The maximum *MNTDR* filter values indicate the edges of the potential anomaly filed. On comparing the mentioned filters, it is worth noting that, due to the nature of the mathematical functions used in their formulae, the *MNTHD* filter returns smoother edges with more hollows, while the *MNTDR* method yields narrower perimeters with relatively more noise. Considering the geological units of the study area and implementing both of the above-mentioned filtering techniques with the use of 3D inversion approaches, a useful vision of the surface projection of the deep and large-scale anomalies can be created.

3. 3D inverse modelling

Inversion is a mathematical problem for obtaining the unknown parameters of a system of equations that leads to the acquisition of physical models of subsurface structures by surveying a set of observed surface data. The physical parameters are often a spatial distribution underneath the Earth's surface. Using the potential field data, the mentioned physical parameters (geophysical density and magnetic susceptibility contrasts) of the model can be calculated based on the potential field theory (Blakely, 1996). Multiple approaches are provided for solving inverse problems. However, one applicable and frequently utilised method is a norm-based Tikhonov regularisation approach (Li and Oldenburg, 1996, 1998).

The initial form of the equation is:

$$P = GM \quad (3)$$

where *P* is the potential field data measured in the geophysical survey, *G* is a linear forward

operator, and M is the physical parameter of the model (geophysical density or magnetic susceptibility of the subsurface structures) with rectangular mesh designed for the surveyed area.

The cost function expression introduced by Li and Oldenburg (1996) consists of a data misfit norm and model stabiliser. The data misfit element reads:

$$\varphi_d = \| w_d(GM - P)\|^2 \tag{4}$$

where the data weighting function (w_d) is a diagonal matrix, which is inversely related to the standard deviation in the i-th datum (σ_i) and given by $w_d = (1/\sigma_1, \ldots, 1/\sigma_N)$ (Li and Oldenburg, 1996).

The norm stabiliser of the model also has the following definition:

$$\varphi_m = \alpha_s \int_v^{\cdot} w_s\{w(r)[M(r) - M_0]\}^2\, dv \;+\; \alpha_x \int_v^{\cdot} w_x \left\{\left(\frac{\partial w(r)}{\partial x}\right)[M(r) - M_0]\right\}^2 dv + \alpha_y \int_v^{\cdot} w_y \left\{\left(\frac{\partial w(r)}{\partial y}\right)[M(r) - M_0]\right\}^2 dv + \alpha_z \int_v^{\cdot} w_z \left\{\left(\frac{\partial w(r)}{\partial z}\right)[M(r) - M_0]\right\}^2 dv \tag{5}$$

where M is the physical property model item, M_0 belongs to the reference model, w_s, w_x, w_y, and w_z are weighting functions, a_s, a_x, a_y, and a_z are coefficients which effect the relative importance of the different factors in the objective function, and $w(r)$ is a depth-weighting function to prevent the retrieved model from focusing on unrealistic depths.

The objective of the inversion is to minimise both data misfit norm and the model stabiliser:

$$\varphi(m) = \varphi_d + \mu\varphi_m. \tag{6}$$

The objective function would be discretised using a finite difference method to obtain:

$$\varphi_m = M^T Z^T W_m^T W_m Z_M \equiv m W_m^T W_m m \tag{7}$$

where $W_m^T W_m$ is the weighting matrix, which indicates the model objective function and Z is the diagonal matrix containing the discretised depth-weighting function. The data misfit is calculated by the χ^2 misfit measure as follows:

$$\varphi_d = (G_M - d_{obs})^T (G_M - d_{obs}) = (G_w m - d_{obs})^T (G_w m - d_{obs}) \tag{8}$$

where d_{obs} is the vector including the measured data. The inversion response is achieved by minimising the object function so as to simultaneously minimise φ_m and φ_d. In general, parameter μ is considered and the following equation is minimised:

$$\varphi(m) = \varphi_d + \mu\varphi_m \quad constraint: m > 0. \tag{9}$$

Worthy of mention is that μ is a regularising parameter that balances the corresponding

importance of each norm and has a crucial role in the final results (Trade-off). The *L*-curve method is a proper approach for estimating the regularisation parameter. The constraint of *m* has been established for the positivity constraint. In the logarithmic barrier method, the positivity constraint is accomplished by means of a logarithmic term. The new objective function is:

$$\varphi(m,\lambda) = \varphi_d + \mu\varphi_m - 2\lambda \sum_{j=1}^{M} \ln(m_j) \tag{10}$$

where $-2\lambda \Sigma_{j=1}^{M} \ln(m_j)$ is the barrier function and λ is the barrier parameter (obtained by a recursive equation in the algorithm), and μ is the regularisation parameter (Li and Oldenburg, 2003).

By solving the above-presented system of equations in this research, the subsurface susceptibility distribution of deep underground structures is obtained as the physical parameters with valid fittings. In recent years, much research has been conducted to solve Eq. 6 (Fournier, 2015, 2019; Azadi *et al*., 2022). In this study, the Li and Oldenburg (1996, 1998) and Oldenburg and Li (2005) inversion algorithms have been employed for the inverse modelling of the potential field data.

4. Geological setting of the Sabzevar ophiolite belt

As one of the prominent ophiolites in Iran, the Sabzevar ophiolite belt is a large-scale complex geological event in continuation of the continental crust of the central Iranian zone. The igneous lithology of the area includes peridotite (dunite and harzburgite), pyroxenite, serpentinite, gabbro, and mafic complexes. Intrusive massive and gabbroic, micro gabbroic, dibasic, and dacitic dykes present outcrops in the Sabzevar complex as well. The sedimentary rocks, which include deep to shallow sea rocks, belong to the Upper Triassic to Lower Cretaceous.

Ophiolites are also defined as oceanic lithosphere components driven to the continental margin by orogenic phenomenon (Coleman, 1967, 1971; Bird *et al*., 1971; Dewey and Bird, 1971).

Generally, from bottom to top, an ophiolite sequence contains the following units:

1) ultra-mafic rock complexes composed of transformed peridotites;
2) peridotite, pyroxenite, and gabbro layers with plagiogranite;
3) a complex of dibasic and doleritic plate dykes;
4) a basic complex, usually forming caprocks on the top of the ophiolite units;
5) overhead sedimentary sections including silicate shales, radiolarian chert, plaggic limestones, and limestone with chert lenses (possibly containing fossils).

The ophiolite belt of Sabzevar extends for over 300 km in length and 30 km in width, with a NW-SE trend, which separates the southern area (Lut block) of the Sabzevar plains from the northern parts of the Jovin plain. In the past, the study area was also investigated by many researchers (Takin, 1972; Alavi-Tehrani, 1976; Lench *et al.*, 1977; Noghreyan, 1982; Baroz *et al*., 1983; Moghadam *et al.*, 2014).

The major sedimentary sequences around the mentioned ophiolite region consist of plaggic limestones along with radiolarite. According to palaeontology, the sediments along the volcanic series belong to the Late Cretaceous. The shale units of the area are mostly green and red.

The igneous body of the study area is the piece of oceanic lithosphere, which includes the upper mantle. Located at the central zone of the study area, the ophiolite sector of the region covers the following geological sequences:

a) enormous masses of harzburgite: formed by the tectonic activities involved with oceanic mantle origination;
b) ultra-basic and layered series of gabbro: a formation caused by basic lava, showing a complete succession of the intermediate rocks such as lherzolite feldspars, gabbro and acidic rocks like quartz diorite and granophyre. Formed by the subtraction of basic magma subtraction in relation to harzburgite masses, these intrusive rocks can be interpreted as a result of a partial melting process within the upper mantle;
c) sheeted dibasic dykes: depending on the mentioned ophiolite sequences, these are the other elements of the igneous rocks of the study region;
d) micro-gabbro units: these are substantial veined stones present in the area. Sea lavas with pillowed formations can be observed within the region; the lithological combination of the mentioned rocks consists of basalt, spilite, and keratophyre.

A part of the ophiolite zone lithology belongs to metamorphic rocks, among which metaophiolites. Geology and petrography studies indicated that the metamorphic complex consists of two dominant parts:

1) the first consisting in a series with a high degree of metamorphism, such as amphiboles and garnets, which relate to deep sections of the lithosphere. Its exposure is caused by tectonic movements;
2) the second consisting in a series including metamorphic pillowed lavas, green shale series, and glaucophane schists related to the orogenic phenomenon.

Previous research on the study area states that the mentioned area is under the influence of two major metamorphic phases (Lench *et al*., 1977):

i) the first phase, also known as the expansion phase, is the phase in which the static metamorphic condition is proportional to the ocean floor; some of the outcomes can consist in serpentinisation, rodingitisation, and probably spilitisation processes;
ii) the second phase, also known as the compressional phase, is related to various types of Alpine orogeny. The results are manifested through high pressure and mediocre temperature. The glaucophane schists are known as the main conclusion of the orogenic phase of the area.

Fig. 2 indicates the ophiolite zone distribution in the Sabzevar-Torbat-e-Heydarieh belt (study area). As illustrated, the area is over 300 km long and is located in the southern part of the Kopeh Daq Mountains and the northern part of the major Dorouneh strike-slip fault, which separates it from the Lut block. According to the map, the area is divided into four formations: 1) ophiolites in the north and west of Sabzevar city, 2) ophiolites that are located in SSW of Sabzevar city, 3) ophiolites north of Torbat-e-Heydarieh, 4) ophiolites in the SW of Neyshabour (Moghadam *et al*., 2014). The Upper Cretaceous lies on the mentioned ophiolites up to Paleocene extrusive rocks, plaggic limestones, volcanoclastic sediments, and radiolarian cherts. The ophiolites in the north of Sabzevar city have formed an ophiolite belt approximately 150 km long and 30 km wide. This belt is a section of the northern part of the Sabzevar ocean, which belongs to the Late Cretaceous era (Şengör, 1990). These ophiolite complexes will be investigated and divided into six ophiolite formations (Fig. 4).

5. Airborne magnetometry investigation

As previously noted, aeromagnetic data were surveyed from 1974 to 1978, under the Geological Survey of Iran (GSI) administration. The survey presented a 7.5-kilometre flight

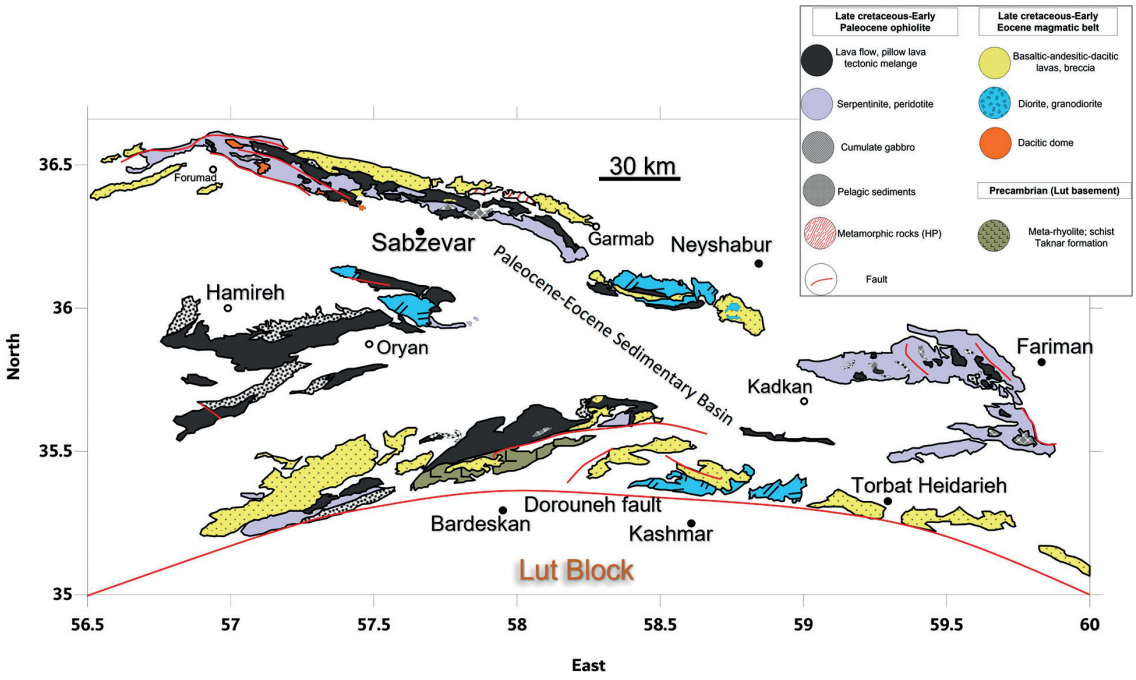

Fig. 2 - Geological map of the Sabzevar-Torbat-e-Heydarieh zone (north of the Dorouneh fault), with considerations on the ophiolite areas (reproduced from Moghadam *et al.*, 2014).

spacing with an altitude from 700 to 3500 m (Yousefi and Friedberg, 1977; Ghobadian *et al.*, 2014). The aeromagnetic data covered most of Iran, but it is worth noting that a partial zone of Kopeh Daq was excluded from the study area (data gap).

Fig. 3 shows the residual map of the airborne magnetic data after subtracting the Earth's

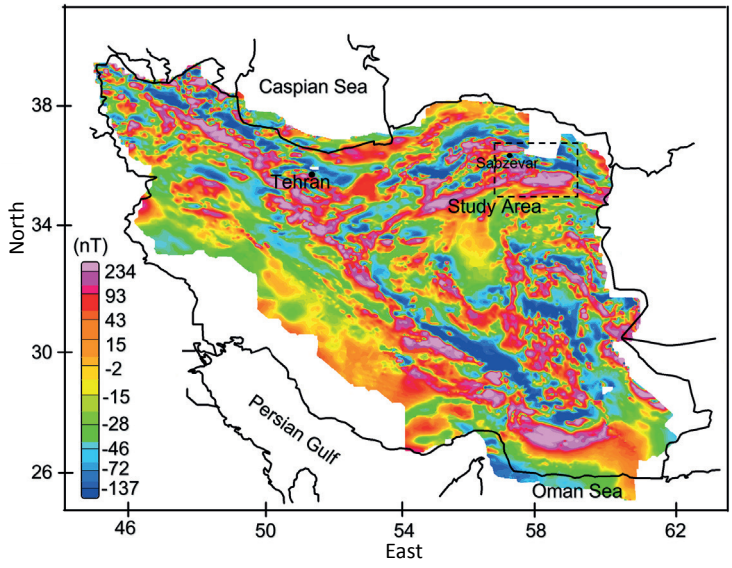

Fig. 3 - Residual map of airborne magnetic data after subtracting the Earth's magnetic field over Iran.

magnetic field over Iran (Saleh, 2006). Evidently, the study area is determined by a rectangular dashed border at the north-eastern quarter of the magnetic grid.

In order to investigate the study area, particularly in terms of geological and magnetic properties, the ophiolite formations are superimposed on the residual and RTP grids. By facilitating the analyses, the RTP filter can dramatically intensify the borders of various structural geological units in tectonic studies (Abedi and Bahroudi, 2016). In addition, the mentioned filter can simplify the interpretation of complicated multi-source magnetic anomalies (Hosseini *et al*., 2021). Fig. 4 portrays the ophiolite geological formations and the related magnetic grids.

As represented, due to their geological and magnetic features, the Sabzevar geological formations are divided into six major areas. The Northern Sabzevar Ophiolite (NSO) exhibits high magnetic intensity (more than 200 nT) in the NW of the magnetic maps, as a consequence of the basaltic-andesitic lavas and lava flows, and in the breccia zones (Fig. 2). Including pelagic sediments, lava flows, diorites, and granodiorites, the Southern Sabzevar Ophiolite (SSO) is located in the middle of the area. As opposed to the NSO, this zone shows from low to high ranges of magnetic intensity. According to previous research, Bardaskan Ophiolite (BO), Neyshabour Ophiolite (NO), and Torbat-e-Heydarieh Ophiolite (THO) formations, that possess analogous lithological properties (a considerable measure of igneous rocks), reasonable and expected magnetic intensity ranges, can be seen in the shown grids (high ranges of magnetic field intensity) (Moghaddam *et al*., 2014).

Conversely, serpentinite and peridotites are among the dominant rocks belonging to the Fariman Ophiolite (FO). Therefore, a medium range of magnetism is plausible. It is worth noting that, due to the orogenic activities, the area presents numerous faults and fractures (Fig. 5). The most significant fault of the area is the Dorouneh fault, separating the northern ophiolite zone from the Lut block, which is also evident in the magnetic grids. Some conspicuous faults in the magnetic grids are considered in geological maps and field investigations. For instance, some faults exist between the BO and THO formations or the faults belong to the NSO formation, representing quite considerable effects on the magnetic grids.

In order to commence supplementary and interpretational steps, various approaches and tools can be utilised; edge detection techniques are among the most applicable and crucial methods for potential field interpretation over large-scale and tectonic studies. Accordingly, in this research, two newly improved and powerful edge detection filters are applied to the aeromagnetic data of the Sabzevar ophiolite to determine the locations and shapes of the magnetic anomalies of the area. By taking advantage of these filters, dependable information about the distribution, position, extension, and geometry of the favourable ophiolite zones can be achieved. However, the interpretation of the edge detection filters and extraction of the anomaly edges will facilitate the division of the area into different blocks, so as to invert the aeromagnetic data more precisely.

MNTHD and *MNTDR* edge detection filters are tools developed for enhancing resolution and reducing false edges. The *MNTHD* filter is beneficial for the achievement of high-resolution edges. In addition, since the *MNTHD* is a derivative-based filter and vertical derivative is utilised only once in its formula, noises are significant, meaning that false edges are substantially decreased or omitted. The *MNTDR* filter is another powerful edge-detection filter that separates narrower edges and illustrates the details of the edges more accurately; however, noise would be reinforced in this filter as a result of using multiple vertical derivatives in the process (Ghiasi *et al*., 2023). Through trial and error, the adjustment parameters of 0.1, for the *MNTHD* filter, and 0.4, for the *MNTDR* filter, were considered in this research. As discussed, the maximum *MNTHD*

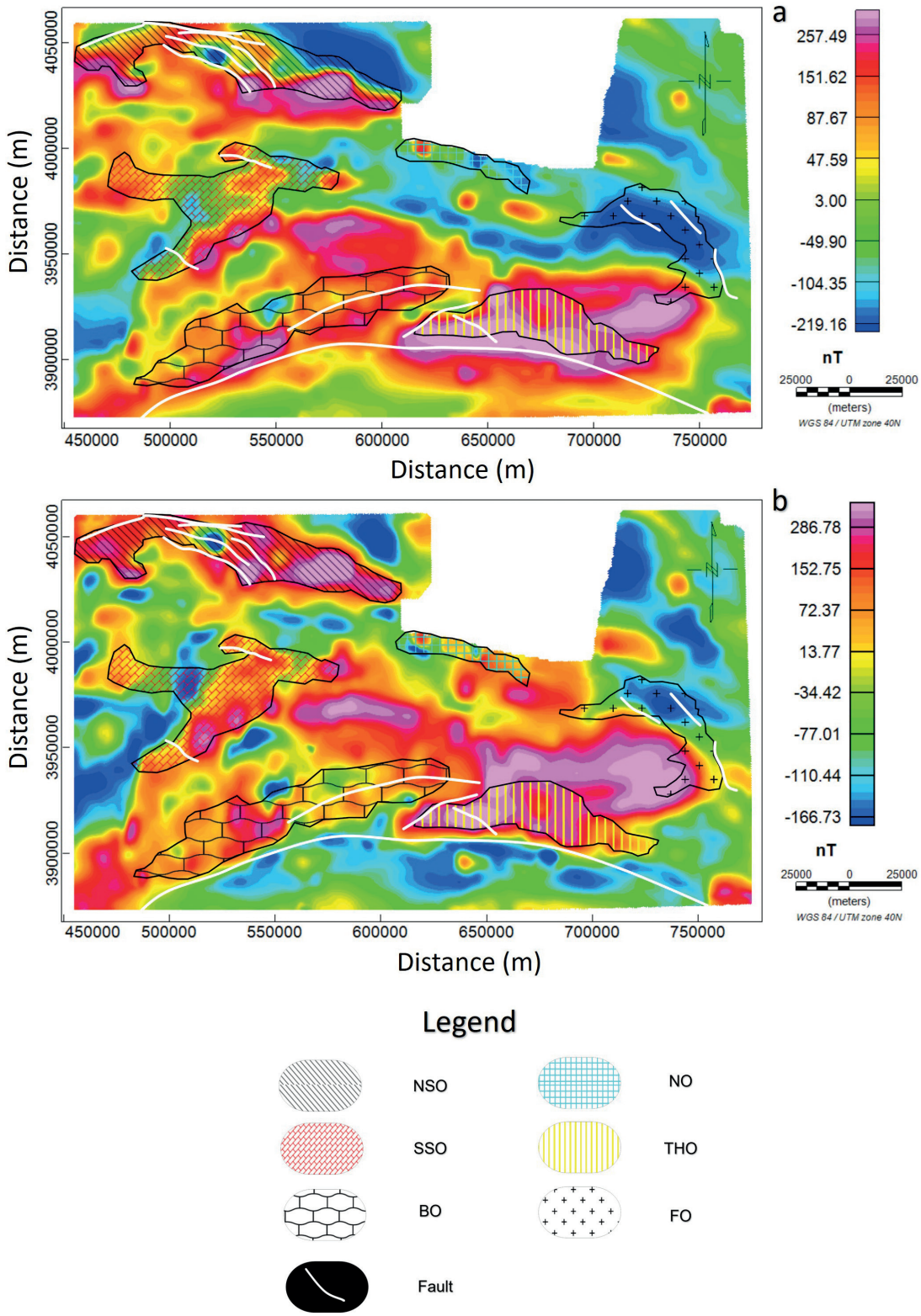

Fig. 4 - Geological formations superimposed over the magnetic grids related to the Sabzevar ophiolite in NE of Iran: a) the residual grid, b) the RTP grid.

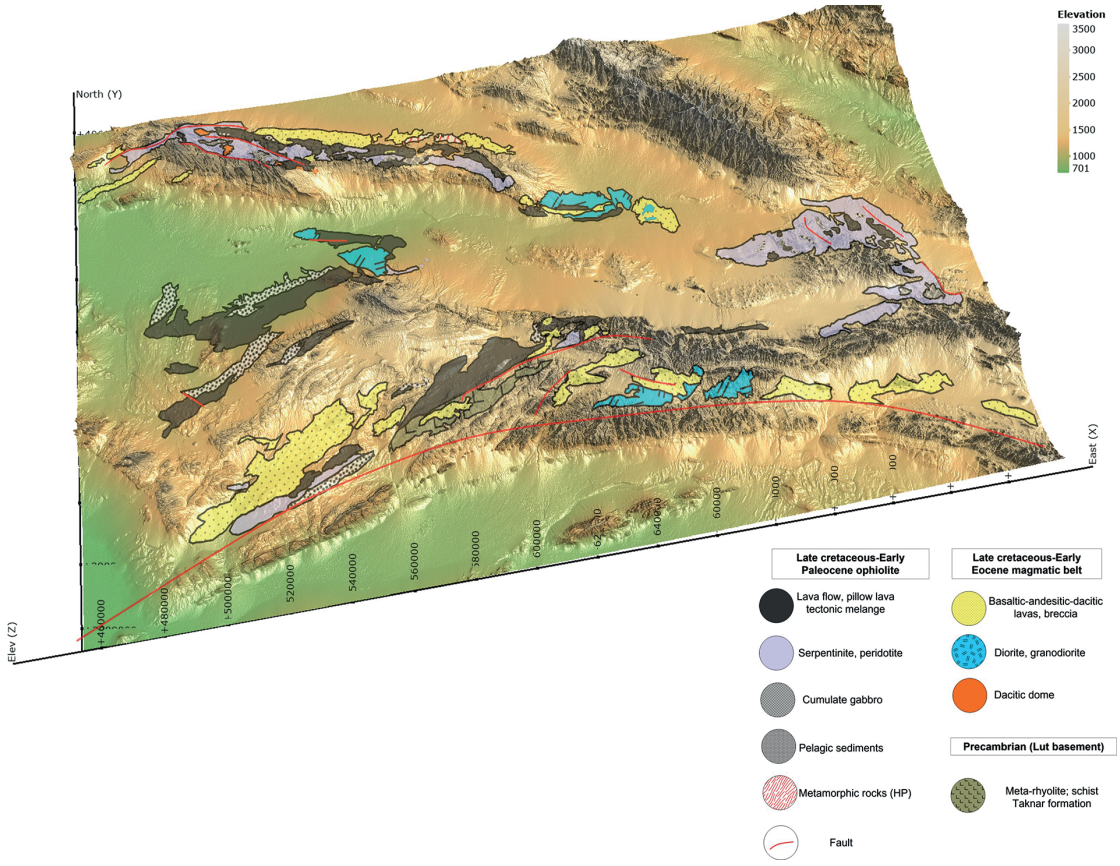

Fig. 5 - Topography map over different geological zones of the Sabzevar ophiolite areas.

and *MNTDR* edge detection filter values represent the boundary of the magnetic anomalies (Ghiasi *et al*., 2023).

Fig. 6a, relevant to the *MNTHD* filter, shows high-resolution edges with substantial relations to each other. Fig. 6b shows the *MNTDR* filter representing more detailed edges and some false edges, which require attention to distinguish the real ones. Hereafter, the edges considered are critical factors in the evaluation of the inverted results for the determination of the ophiolite zones.

As aforementioned, working with edges would boost the interpretation in terms of locating the desirable anomalies; also, in addition, authentic edge detection can be used as a comparison factor to inversion results (Ghiasi *et al*., 2023). Therefore, to create a proper vision, the edges captured from the *MNTHD* and *MNTDR* filters are exhibited with dark blue and sky blue polygons, respectively (Fig. 7a). The black polygons are related to the geological map of the Sabzevar ophiolite zone (Fig. 2). The simultaneous utilisation and consideration of the geological information, along with the anomaly edges from the *MNTHD* and *MNTDR* filters, can be an advantageous summary interpretation. Based on Fig. 7a, it can be observed that the location and shape of the polygons obtained from the edge detection filters show a logical and obvious accommodation with the surface geological complexes. As discussed above, the geological complexes in Fig. 2 are related to the igneous and ophiolite formations across the Paleocene-Eocene sedimentary basin, manifested by the anomaly edges indicated by the polygons. It is worth noting that some high magnetic areas were identified from RTP and edge detection maps with high susceptibility

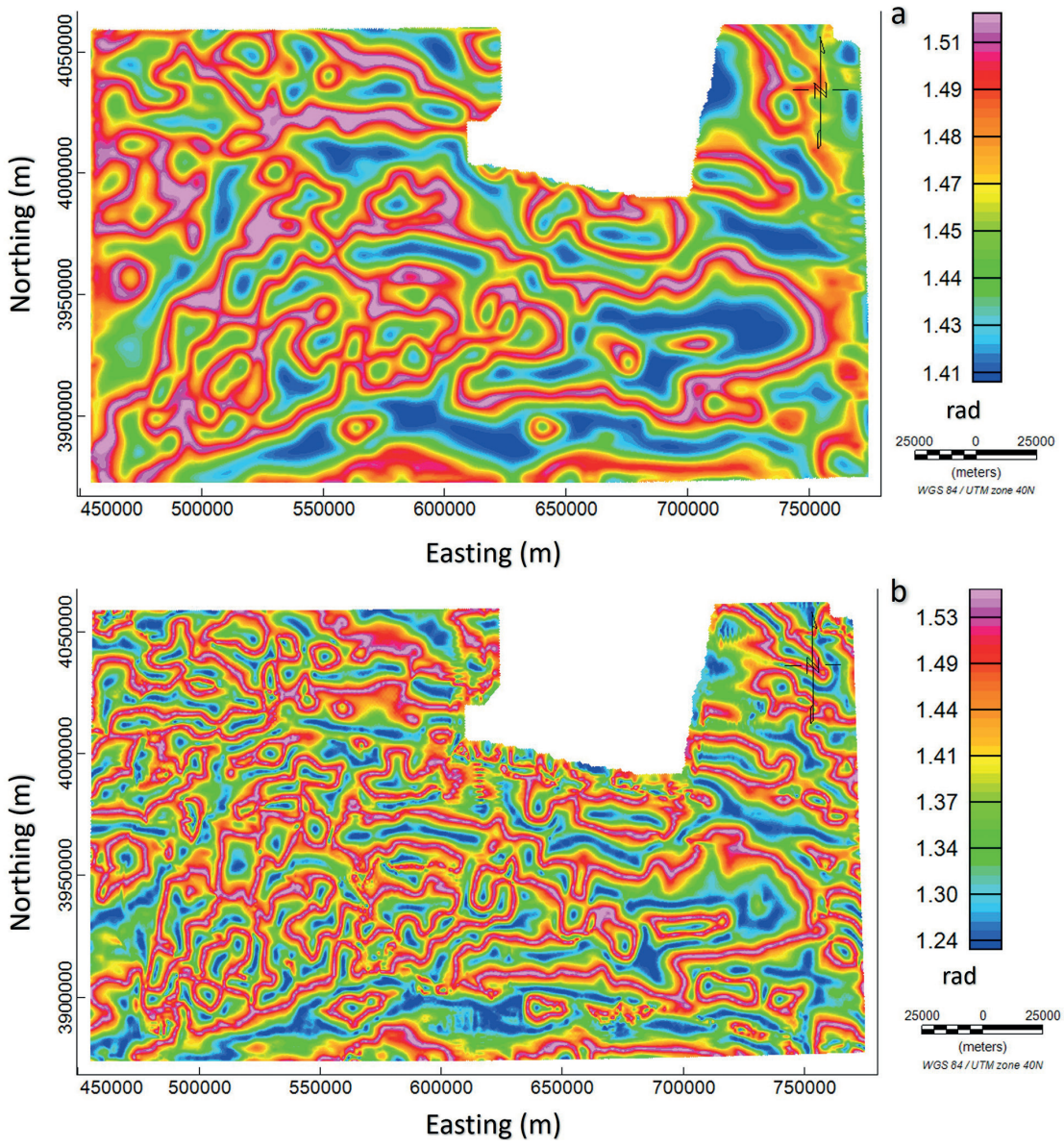

Fig. 6 - The edge detection filters on the RTP magnetic grid: a) the *MNTHD* filter, b) the *MNTDR* filter.

potentials. However, no outcrop manifestation is evident on the existing geological maps. It may also be related to the deep fertile mantle with no outcrop for geological and geochemical investigations. Subsequently, these areas will be studied in detail hereafter. Fig. 8 illustrates the *MNTHD* and *MNTDR* filters on the upward continuation filters of the study area at altitude levels of 20,000, 40,000, and 60,000 m, respectively. The figure facilitates the interpretation of the magnetic source variation by penetrating depths. In addition, Fig. 9 belongs to the *MNTHD* and *MNTDR* filter on upward continuation filters of an area with no surficial exposure. Conversely, the magnetic grids portray the anomaly (block 3 in the inversion section). Fig. 9 correctly shows the depth expansion of the mentioned magnetic source. Figs. 8 and 9 will be compared with the inversion results hereafter, so as to investigate the accuracy of the inversed models.

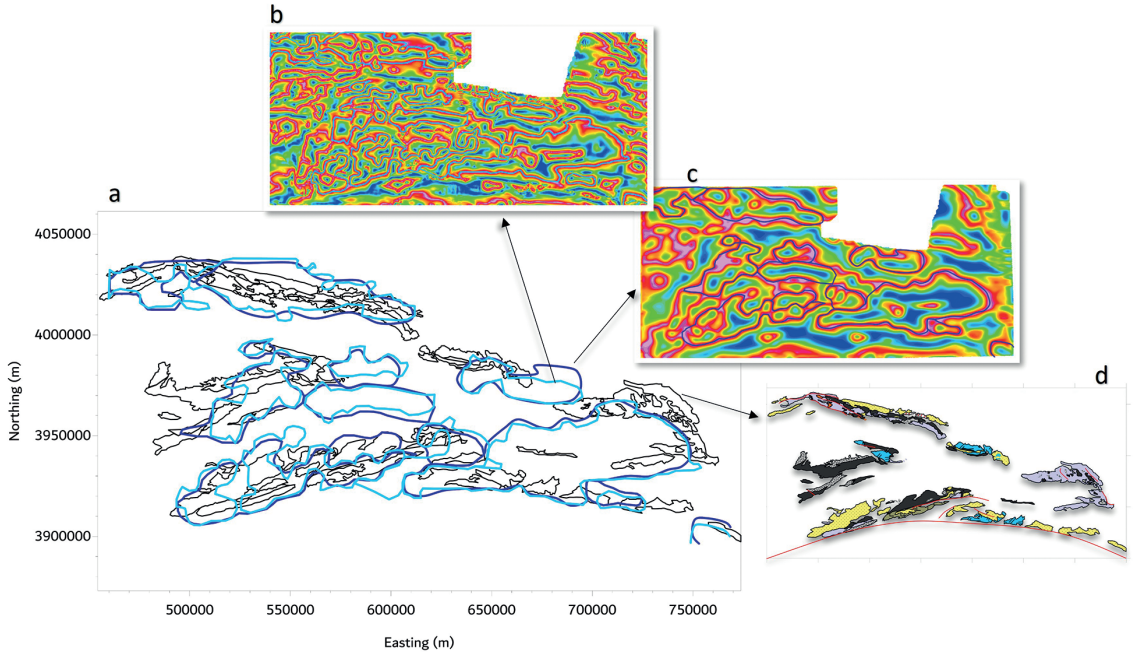

Fig. 7 - The polygonal display of the extracted edges (a) from the *MNTDR* filter (b), the *MNTHD* filter (c), and geological map of the Sabzevar ophiolite complex (d).

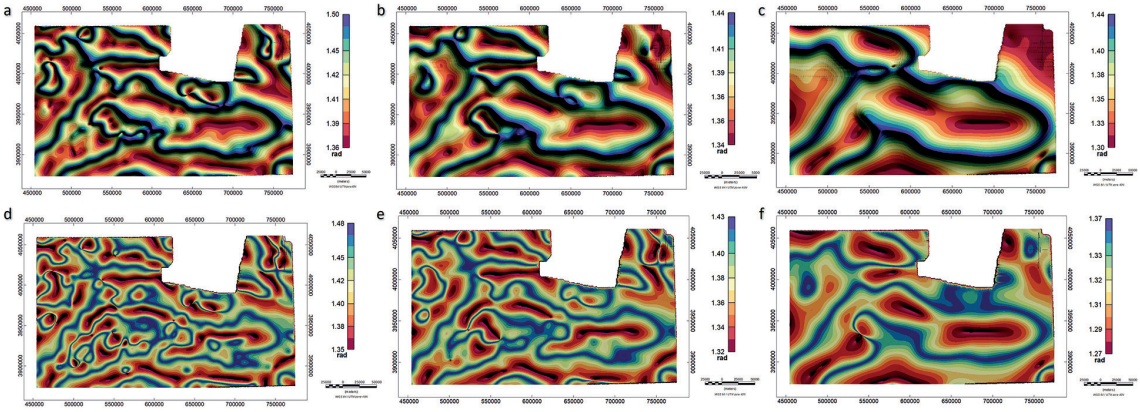

Fig. 8 - The *MNTHD* filters (first row) and the *MNTDR* filters (second row) applied on the upward continuation filters of the entire study area, at three levels of altitude: a) the *MNTHD* filter on a level of 20,000 m, b) the *MNTHD* filter on a level of 40,000 m, c) the *MNTHD* filter on a level of 60,000 m, d) the *MNTDR* filter on a level of 20,000 m, e) the *MNTDR* filter on a level of 40,000 m, and f) the *MNTDR* filter on a level of 60,000 m.

6. Inverse modelling and interpretation

In order to carry out an exhaustive investigation for the study of ophiolites, the aeromagnetic data were inverted to restore the susceptibility contrast model. The combination of the edge detection filters and the mentioned physical model can expedite the interpretation and explanation of the large-scale researches, such as ophiolite cases and tectonic investigations.

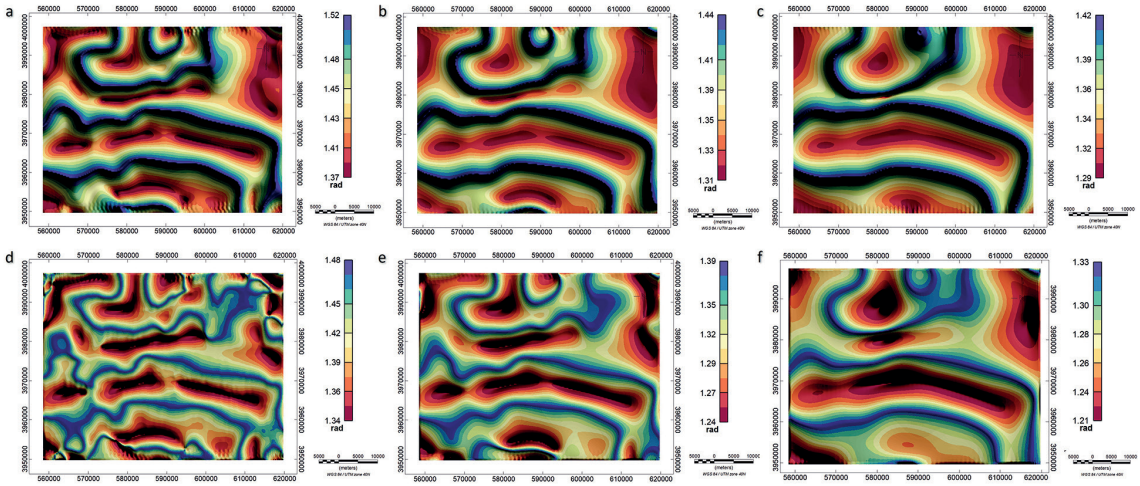

Fig. 9 -The *MNTHD* filters (first row) and the *MNTDR* filters (second row) applied on the upward continuation filters of block 3 at three levels of altitude: a) the *MNTHD* filter on a level of 10,000 m, b) the *MNTHD* filter on a level of 20,000 m, c) the *MNTHD* filter on a level of 30,000 m, d) the *MNTDR* filter on a level of 10,000 m, e) the *MNTDR* filter on a level of 20,000 m, and f) the *MNTDR* filter on a level of 30,000 m.

The magnetic data observed over the study zone was resampled from the gridded data with a spacing from 3 to 4 km, depending on the block dimension, in both the eastern and northern directions. Most of the ophiolite zones are located over the rugged topography and high altitudes (>2 km), originating from orogenic activities. However, the SSO formation is spotted on the smooth topography (<1.5 km) with mediocre altitude in the study area (Fig. 5). It should be noted that, due to the vastness of the study area, an accurate inversion with tight meshes and a small sampling space for the observed data is improbable. Thus, the study area is divided into seven smaller zones called blocks in this study. Creating blocks and subareas in such large-scale cases helps to increase precision and detail. This division makes it convenient to utilise a data set that is more closely observed and a tighter mesh for obtaining accurate inversion results.

Figs. 10, 11, and 12 represent the divided blocks for the 3D inverse modelling procedure and the relevant observed and predicted maps for the comparison and determination of the inversion precision. As illustrated, the study area is divided into seven significant blocks chosen

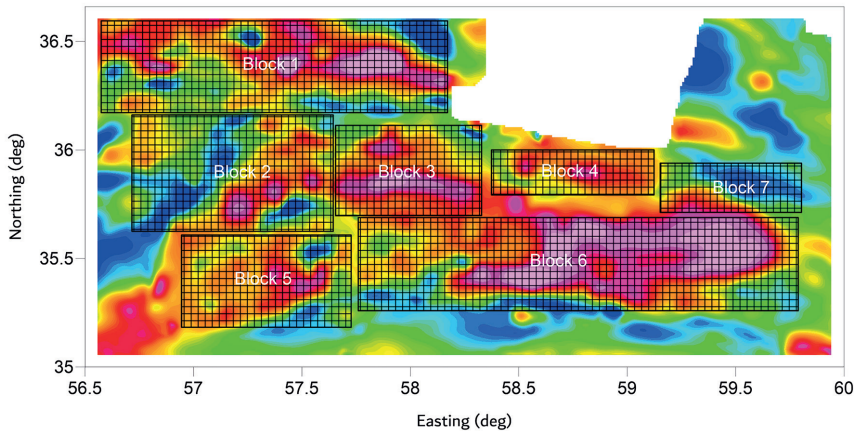

Fig. 10 - Division of the study area into seven separate blocks with various dimensions (according to the edge detection results). The aeromagnetic data were independently inverted, and, eventually, the inverse modelling results were merged. Initial parameters for inverse modelling were similar to each block.

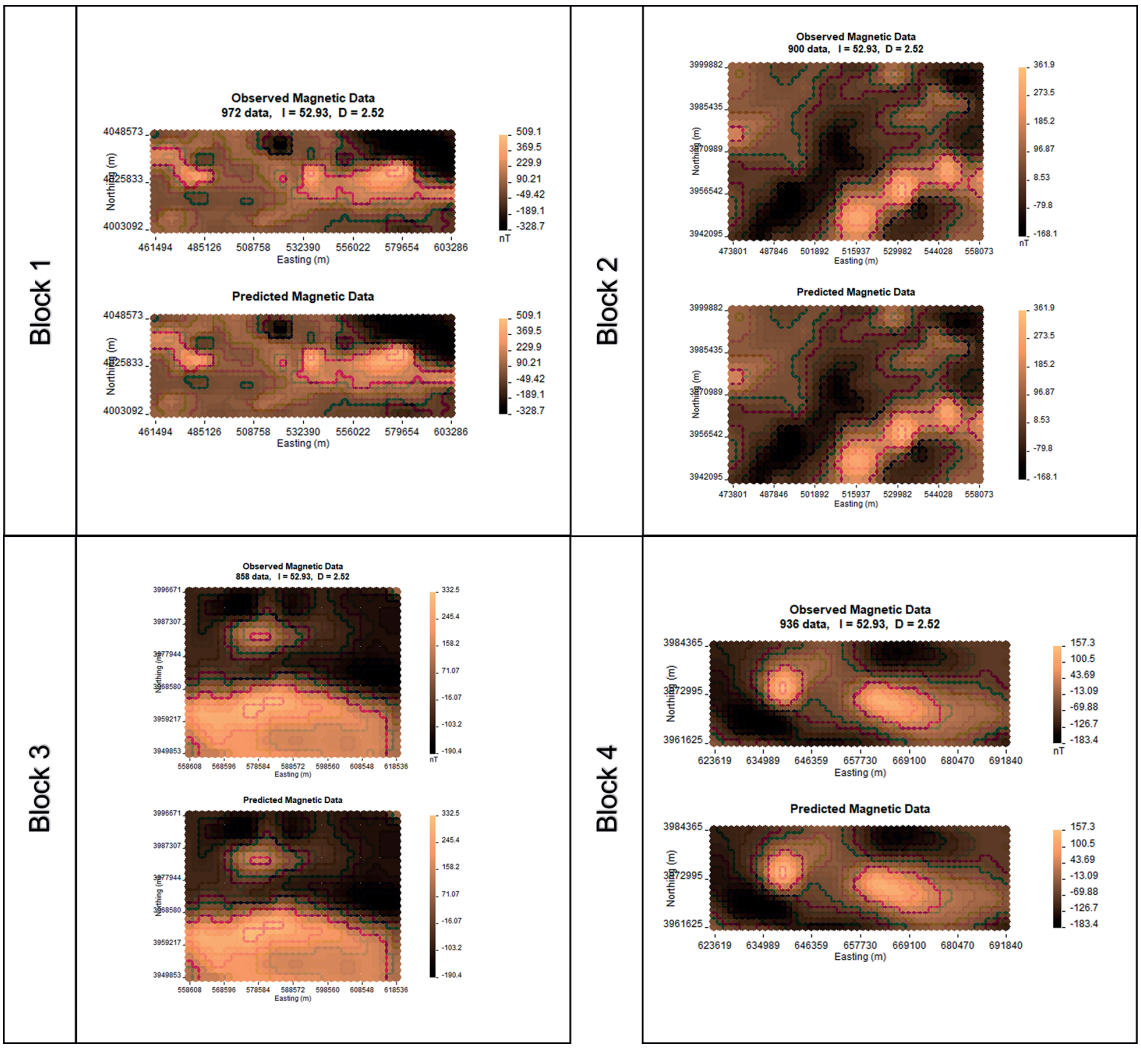

Fig. 11- Observed and predicted grids of the inversion blocks delineating proper misfit for the 3D inverted models (blocks 1 to 4).

by considering the area's edge detection filter results and geological map. The blocks have been separately inverted, and the meshing and data sampling carried out proportionally to the dimensions of each block. The magnetic data for blocks one to seven include 972, 900, 858, 936, 748, 870, and 900 points, respectively. The magnetic data possesses a regular 52.93° inclination, 2.52° declination, and an intensity of 35,999 nT of the Earth's magnetic field. For the allocation of uncertainties, as input for the inversion, a minimum value of 10 nT and 2% of the data amplitude were applied. The designed meshes, which spatially cover the entire related block, have average dimensions of 700×700×400 m^3, to the east, north, and depth direction. For a better visualisation, the blocks over the topography have been discarded from the inversion model. According to the above figure, the observed and predicted data indicate acceptable accommodation; besides, the RMS values are less than one in each inverted block, and the coefficient of determination is approximately one. These factors illustrate the accuracy of the implemented inversion scheme, which is reliable for interpretational purposes. The values of 0.0001 for α_s and 1 for α_x, α_y, and α_z

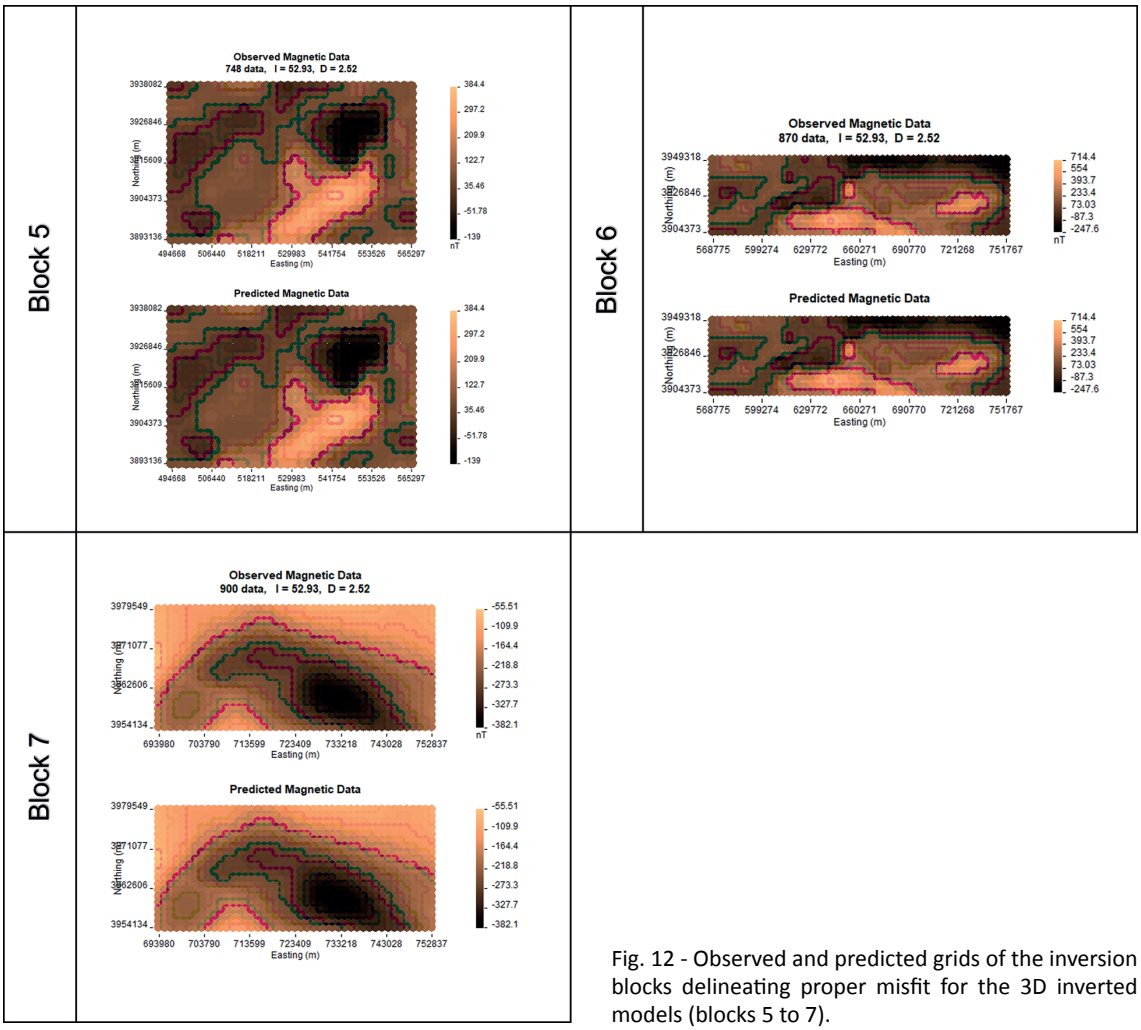

Fig. 12 - Observed and predicted grids of the inversion blocks delineating proper misfit for the 3D inverted models (blocks 5 to 7).

have been considered (recommended by Li and Oldenburg, 2003). Also, regarding the *L*-curves obtained from the inversion procedures, values of 3.45, 4.34, 4.16, 3.78, 2.96, 1.26, and 3.35 have been chosen for the regularisation parameters in each block, respectively. Worthy of note is the fact that, in order to reduce the uncertainty degree and non-uniqueness of the magnetic data inversions, the calculated susceptibility information of igneous rocks in central Iran, with the igneous and ophiolite zone closest to the study area, was employed. Therefore, the mentioned data have been used to bind the susceptibility of each block and build the proportional initial model for inversions, according to the major lithological structure of each block. The susceptibility ranges of igneous rocks are illustrated in Table 1.

It is known that the edge perimeters obtained from processed magnetic grids can reliably expose the realistic features of the physical model beneath the surface. Consequently, the analogy of the edge detection results and magnetic susceptibility models can be a dependable method for approving the inverted model as a precise presentation of the actual geophysical status.

In order to acquire a 3D magnetic susceptibility model of the subsurface structures from aeromagnetic data, the UBC-GIF Mag3D software has been utilised (Li and Oldenburg, 1996,

Table 1 - Magnetic susceptibility statistics for different types of igneous rocks in central Iran (Moghaddam *et al.*, 2022).

Rock type	Lithology	Magnetic Susceptibility (k, 10^3 SI)		Mean of each type
		Range	Mean	
Mafic-ultramafic rock	Ultramafic	25-172	54	48
	Magnetite	42-550	189	
	Peridotite	20-146	76	
	Pyroxenite	20-115	83	
	Gabbro	20-105	37	
	Diabase	30-98	24	
Intermediate-felsic rocks	Diorite	7-97	19	14
	Syenite	5-79	41	
	Granite	0-44	5	
	Granodiorite	0-51	6	
Volcanic rocks	Basalt	12-178	28	19
	Trachyte	10-270	9	
	Andesite	10-188	21	
	Rhyolite	0-68	12	
	Tuff	0-130	16	

1998, 2003). Fig. 13 represents the inverted models of blocks one to four, whereas the *MNTHD* and *MNTDR* edge detection filters are superimposed on the susceptibility models. As mentioned, dark blue and sky blue polygons belong to *MNTHD* and *MNTDR* edges, respectively. For all the 3D models, miniature values of susceptibility have been ignored to effectively display the underground geophysical model. As shown, all the models show proper reconciliation with their obtained edges. Relatively higher susceptibility values in the 3D inverted model, representing the igneous and ophiolite zones, have precisely and substantially influenced the magnetic grids and edge detection filters, as expected. Therefore, it is approved that the properties of the achieved inverted models, in terms of shape, geometry, position, and susceptibility, are applicable to the tectonic studies of the area. It is worth noting that the magnetic edge detection grids in block three showed anomaly zones in that area. However, the geological map of the area did not specify igneous or ophiolite outcrops. Hence, block three was assigned as a target for further complementary investigations. In addition, the susceptibility modelling results countenanced the edge detection maps by the average interval of 0.03 to 0.07 (SI) susceptibility. Consequently, the explored high susceptibility mass, which may relate to ophiolite structures, is a deeply rooted complex (from approximately -2.5 to 18 km) with no outcrop on the surface, so geological and geochemical studies may not be able to properly search downwards into it. Accordingly, the mentioned area can be considered as a highly susceptible zone, igneous and probably an ophiolite complex.

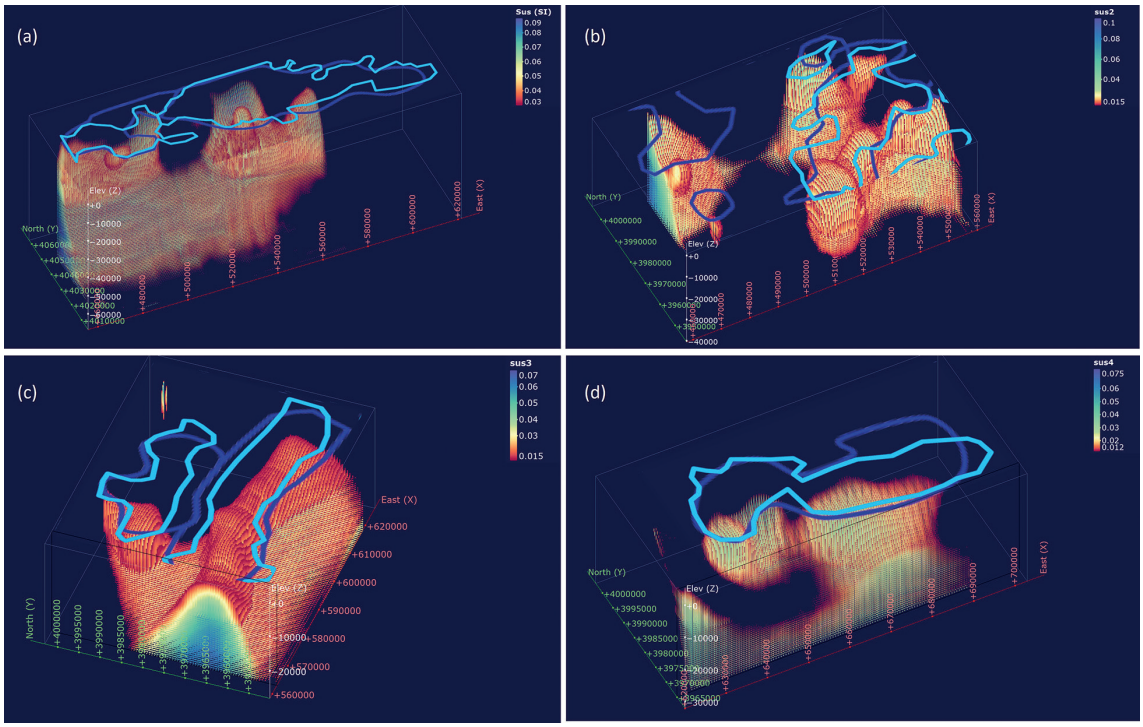

Fig. 13 - 3D inverted susceptibility models of the Sabzevar ophiolite zone overlaid with the *MNTHD* (dark blue polygons) and *MNTDR* (sky blue polygons) filters for: a) block 1, b) block 2, c) block 3, and d) block 4.

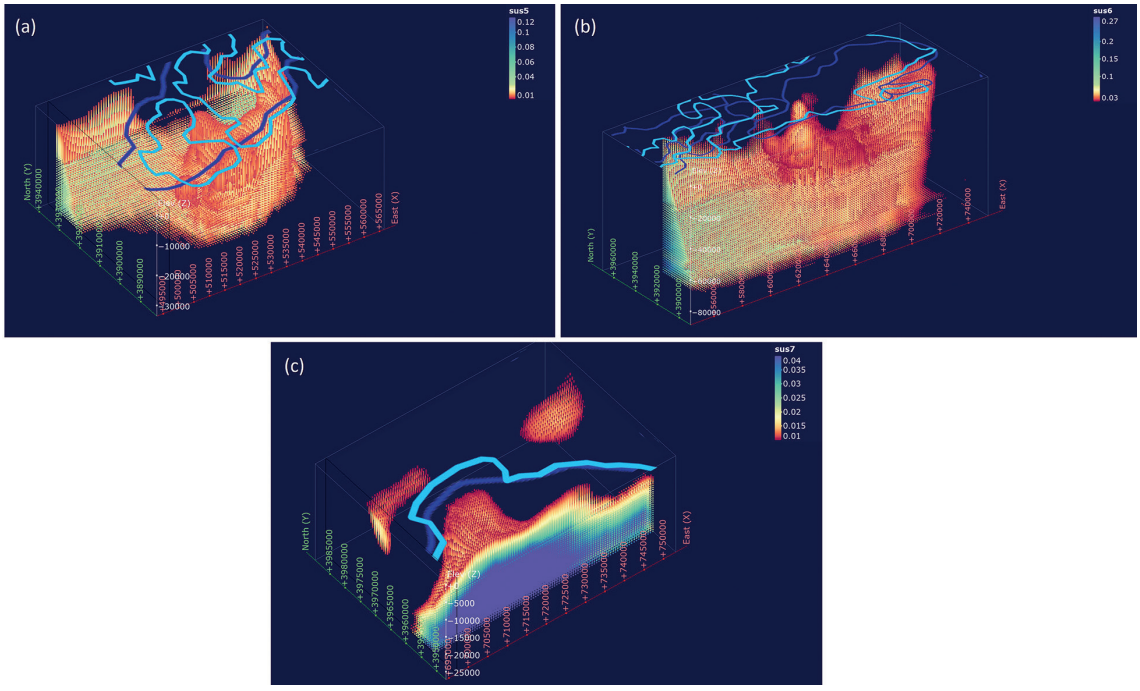

Fig. 14 - 3D inverted susceptibility models of the Sabzevar ophiolite zone overlaid with the *MNTHD* (dark blue polygons) and *MNTDR* (sky blue polygons) filters for: a) block 5, b) block 6, and c) block 7.

Fig. 14 demonstrates the 3D inverse modelling results for the rest of the blocks, i.e. the fifth, sixth, and seventh. Of note is the fact that the small susceptibility values are left out so as to represent the model in a sharper manner. It is obvious that the geometry and the position of the 3D susceptibility models are congruous with their *MNTHD* and *MNTDR* filters, which state reliable inversion results.

Here following, 2D contour sections of the 3D susceptibility models, on the XY and YZ planes, have been utilised to clearly represent the orientation gradient of the susceptibilities.

As illustrated, Fig. 15 belongs to the 2D contour sections on the XY and YZ planes for blocks one to four. The medium to high susceptibility zones are clearly shown in the cited figure. Accordingly, Fig. 16 depicts the 2D contour sections on the XY and YZ planes of blocks five to seven. It must be said that the presentation of the contour sections would help the interpreter to characterise the internal details and changes in the 3D susceptibility model. As is evident, the dominant trend of the model belongs to the growth of the susceptibility values with increasing depth in the ophiolite zones. Due to the existence of mediocre susceptibility values near the surface in the fractured zones, faults of the study area control the lava penetration at shallow levels. By comparing the susceptibility distribution obtained from the inversion method in Figs. 15 and 16, using magnetic sources at different depths (Figs. 8 and 9), susceptibility values and magnetic intensities are perceived to be correlated, thus representing the precision of inversions.

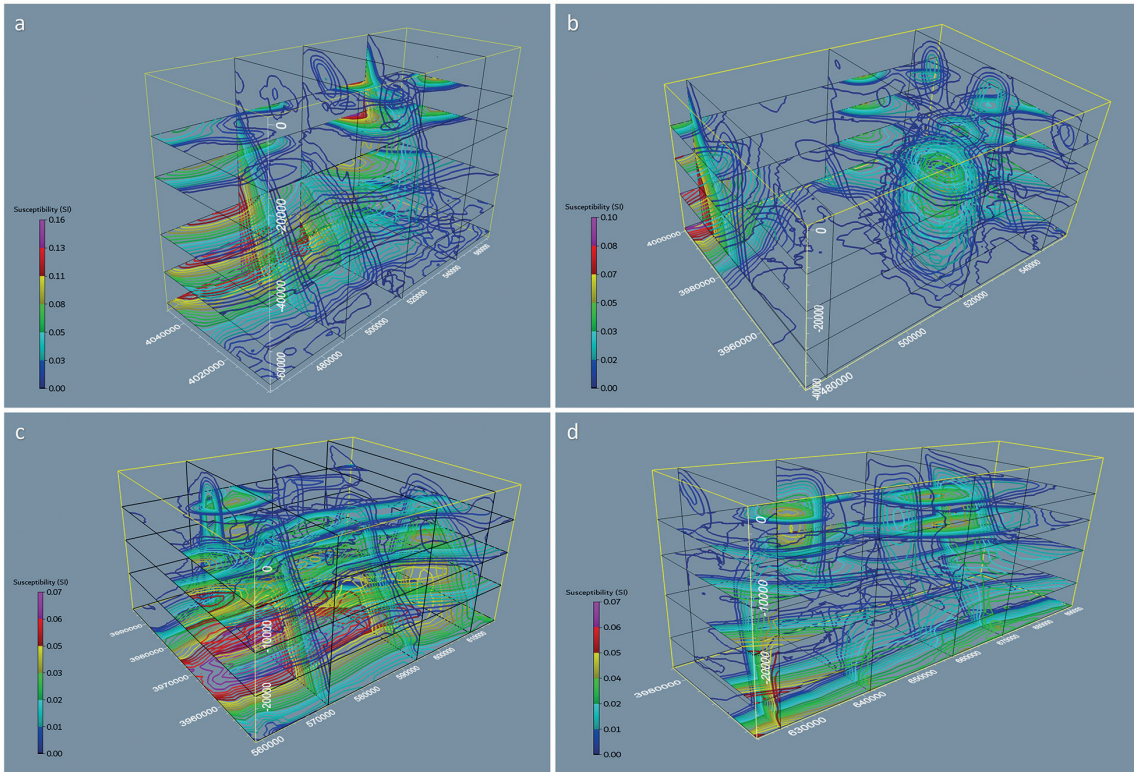

Fig. 15 - 2D contour sections over 3D inverted susceptibility models of the Sabzevar ophiolite zone for the XY and YZ plane sections of: a) block 1, b) block 2, c) block 3, and d) block 4.

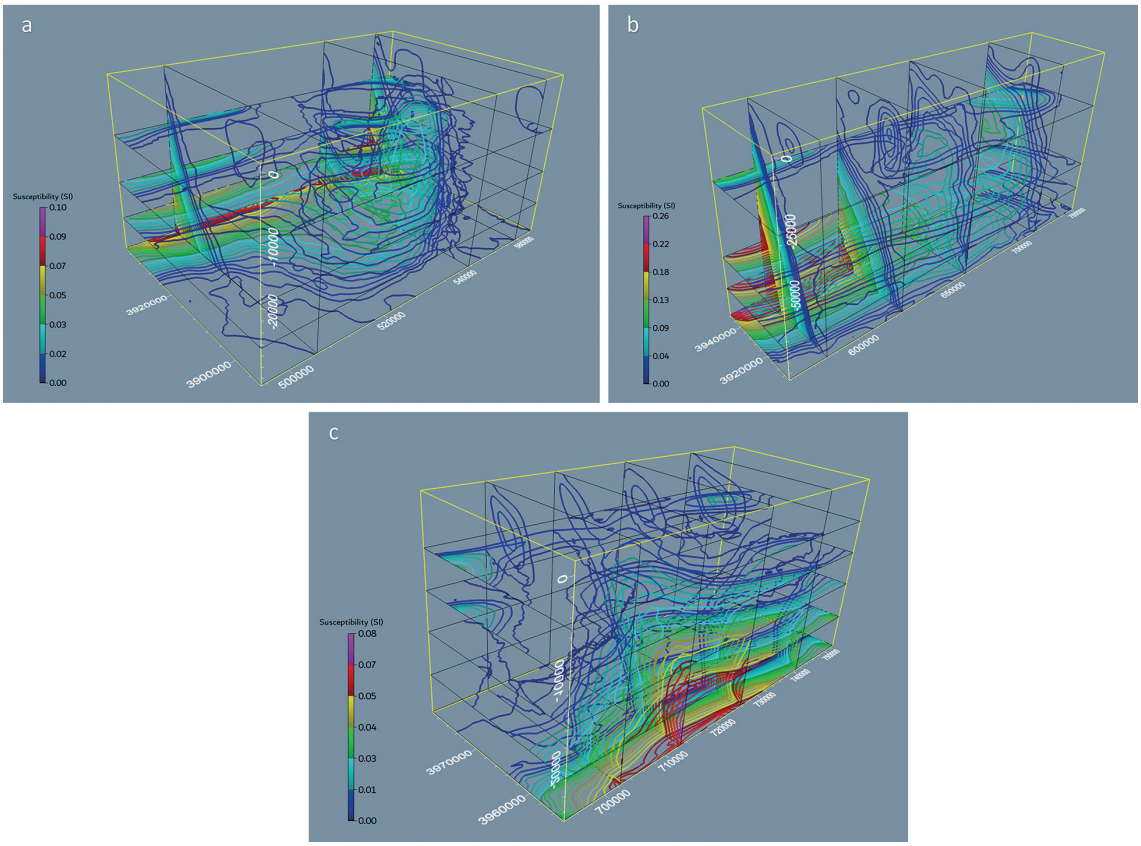

Fig. 16 - 2D contour sections over 3D inverted susceptibility models of the Sabzevar ophiolite zone for the XY and YZ plane sections of: a) block 5, b) block 6, and c) block 7.

7. Discussion

Ophiolite areas are believed to form in subducted and orogenic zones; therefore, highly elevated lands in the study area were pre-predicted. A classic sequence of oceanic lithosphere includes ultramafic rocks and serpentinite at the bottom of the sequence, as well as gabbro and basalt, and chert or turbidite at the top of the series. Therefore, a range of susceptibility values increasing with greater depth would be plausible for typical ophiolite formations. As previously discussed, the leading purpose of this work was to investigate and study the NE ophiolite area of Iran, in terms of tectonic aspects and characterisation of the deep structures. To meet these objectives, two recently improved edge detection filters were exploited, and the results were also combined and overlaid with the outputs of the 3D inverse modelling algorithm to achieve persuasive interpretations. As expected, the edge detection outcomes from the *MNTHD* filters returned high resolutions, and the *MNTDR* illustrated narrower edges with more detail as well as normal noise and few false edges. Overall, the aeromagnetic grids have perfectly portrayed the geological features and magnetic anomalies. Main faults are evident within the magnetic maps; for instance, through the most significant faults in the study area, the Dorouneh fault, together with the NSO and SSO faults, can be seen in the magnetic grids (Fig. 4). The complementary interpretative method, to identify the subsurface structure in terms of magnetic susceptibility,

would be 3D inverse modelling of the aeromagnetic data within the study area. Some distinct displacements, with equivalent susceptibilities, lead to the formation of furrows in the first and second inverted model blocks (Figs. 13a and 13b). Through additional investigation, the mentioned displacements are understood to have meaningful accommodation, with the geological faults, in their position (Fig. 4b). For this reason, due to the 3D inverted models, the 15-kilometre depth, on average for faults in block one, and 18-kilometre depth, in block two, were considered. The consolidation of simultaneous utilisations of surface 2D edge detection results and 3D inverse modelling of subsurface structures can validate the conclusions as the 2D edge grids are products of the 3D susceptible anomaly structure outcomes underneath the surface of the Earth. Accordingly, the evident matching of the edge detections and inverted models of the blocks confirm the inversion accuracy. Considering the typical ophiolite sequence, in most of the previous areas, the susceptibility values increase with the increase of penetration in depth, and non-susceptive areas correspond to the sedimentary units such as the Paleocene-Eocene sedimentary units. In addition, the non-susceptible units of the primary layers over the blocks, which have been excluded in the inverted models, are mainly related to thick Paleocene to Eocene conglomerates, turbiditic sequences, and Late Cretaceous limestones (Moghadam *et al*., 2014). The secondary layers of the Sabzevar ophiolite series, divided into crustal and mantle sequences, respectively, are related to Late Cretaceous ophiolites. Thus, this fact satisfies the greater susceptibility values in deeper levels.

As a consequence, the relatively high susceptibility model of the entire study area is presented in Fig. 17. In this figure, only the highest susceptibility values are qualitatively illustrated to facilitate the location of the most critical zones for purposes of prospective studies. In order to distinguish the high susceptibility zones of each block, various spectra of colours have been employed to present the model; thus, the colours are not related to the quantity of susceptibility. Fig. 17 shows the high susceptibility zones from four points of view that comprehensively specify the geometry and expansion of the favourable zones. Fig. 17e highlights the high susceptibility zones, which are illustrated in Figs. 17a to 17d with integrated overlaying of the RTP, edge detection, and ophiolite zones of the study area. As previously discussed, the finalised model of the magnetic properties of the Sabzevar-Torbat-e-Heydarieh ophiolite belt can provide a fundamental perspective to the complementary geophysical exploration.

8. Conclusions

This project was undertaken to design consistent geophysical interpretations, and to evaluate the previous geological survey in the Sabzevar ophiolite complex, for the first time. As discussed, the airborne magnetic survey can be a satisfactory choice for tectonic and ophiolite study over the NE ophiolite zone of Iran, where the orogeny and subduction phenomena are evident. The integrated interpretation of 2D edge detection filters and 3D inverse modelling results could accurately characterise the igneous and feasible formations in the study area, so that the results would be a valuable infrastructure for more detailed investigations in this area. As expected, the edge detection results, which were achieved through the use of geological maps, have identified the different complexes of the igneous and ophiolite rocks in the vast study area. The susceptibility model also showed suitable accommodation with the ophiolite and tectonic sequence of the study area, which was obtained from geological and geochemical research. The low susceptibility values are related to sedimentary units, and increased susceptibility values correspond to the crustal and mantle sequence of ophiolites. The growth of the susceptibility

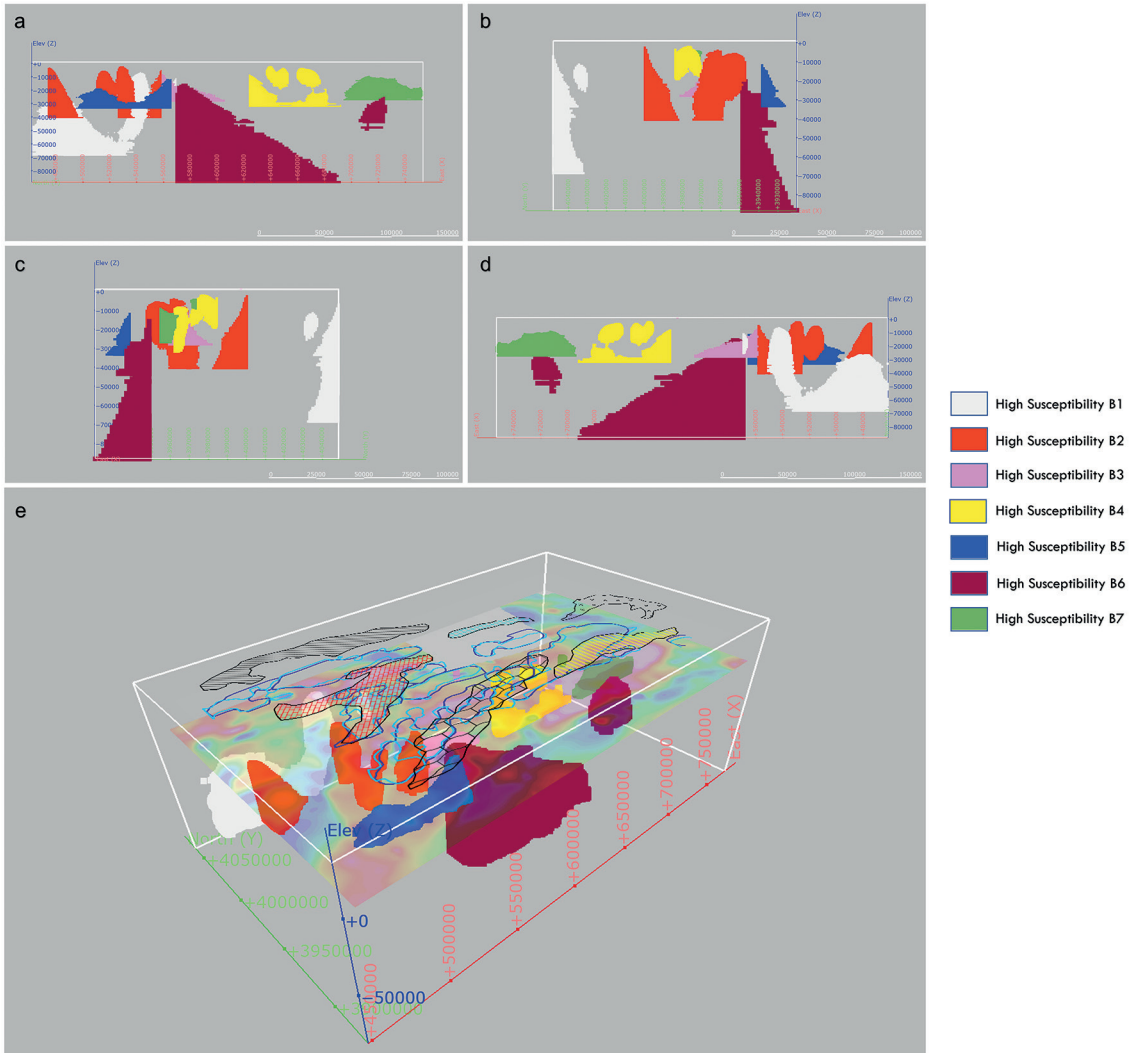

Fig. 17 - Highly susceptible intrusions beneath the Sabzevar ophiolite zone for seven inverted blocks from four points of view: a) front (north), b) left (east), c) right (west), d) rear (south), and e) 3D model of the Sabzevar ophiolite area overlaid by RTP, edge detection filters, and ophiolite complexes of the region.

values by penetrating in depth is evident in 2D section figures. In addition, the high susceptibilities in the shallower standings are related to the faulted structures which help lavas in penetrating upwards. In conclusion, the aeromagnetic data grids, edge detection maps, and 3D susceptibility models characterise the magnetic properties of the Sabzevar ophiolite zone to a degree that the deep expansion of the auspicious area, the faults, and the susceptibility distribution in the Sabzevar-Torbat-e-Heydarieh ophiolite belt have been properly determined through novel interpretational perspectives.

Acknowledgments. The authors express their sincere thanks to the Institute of Geophysics and the School of Mining Engineering, University of Tehran, and to the Department of Mining and Metallurgical Engineering, Amirkabir University of Technology for all the support provided.

REFERENCES

Abedi M. and Oskooi B.; 2015: *A combined magnetometry and gravity study across Zagros orogeny in Iran*. Tectonophys., 664, 164-175.

Abedi M. and Bahroudi A.; 2016: *A geophysical potential field study to image the Makran subduction zone in SE of Iran*. Tectonophys., 688, 119-134.

Alavi-Tehrani N.; 1976: *Geology and petrography in the ophiolite range NW of Sabzevar (Khorassan: with special regard to metamorphism and genetic relations in an ophiolite suite).* Thesis in Geophysics, University of Saarbrücken, Germany, 147 pp.

Azadi M., Abedi M. and Norouzi G.H.; 2022: *Two-step inversion of airborne geophysical data: a stable downward continuation approach for physical modelling*. Acta Geophysica, 70, 121-139.

Baroz F., Macaudière J., Montigny R., Noghreyan M., Ohnenstetter M. and Rocci G.; 1983: *Ophiolites and related formations in the central part of the Sabzevar range (Iran) and possible geotectonic reconstructions*. In: Madelet V. (ed), Geodynamic project (Geotraverse) in Iran, Geological Society of Iran, Report n. 51, Tehran, Iran, pp. 51-68.

Baroz F., Macaudière J., Montigny R., Noghreyan M., Ohnenstetter M. and Rocci G.; 1984: *Ophiolites and related formations in the central part of the Sabzevar range (Iran) and possible geotectonic reconstructions*. N. Ib. Geol. Paläont. Abh. 168, 358-388, doi: 10.1127/njgpa/168/1984/358.

Bird J.M., Dewey J.F. and Kidd W.S.F.; 1971: *Proto-Atlantic oceanic crust and mantle: Appalachian/Caledonian ophiolites.* Nature, 231, 28-31.

Blakely R.J.; 1996: *Potential theory in gravity and magnetic applications*. Cambridge University Press, Cambridge, UK, 441 pp.

Brongniart A.; 1821: *Sur le gisement ou position relative des ophiolites, euphotides, jaspes, etc. dans quelques parties des Apennins.* Huzard, Paris, 64 pp.

Coleman R.G.; 1967: *Low-temperature reaction zones and Alpine ultramafic rocks of California, Oregon, and Washington.* USGS Bull*.,* 1247, 49 pp., doi: 10.3133/b1247.

Coleman R.G.; 1971: *Plate tectonic emplacement of upper mantle peridotites along continental edges*. J. Geophys. Res., 76, 1212-1222.

Coleman R.G.; 1977: *Ophiolites: ancient oceanic lithosphere.* Springer-Verlag, New York, NY, USA, Minerals and Rocks, vol. 12, 239 pp.

Cordell L. and Grauch V.J.S.; 1985: *Mapping basement magnetization zones from aeromagnetic data in the San Juan basin, New Mexico*. In: Hinze W.J. (ed), The utility of regional gravity and magnetic anomaly maps, Society of Exploration Geophysicists, Houston, TX, USA, pp. 181-197, doi: 10.1190/1.0931830346.ch16.

Desmons J. and Beccaluva L.; 1983: *Mid-ocean ridge and island-arc affinities in ophiolites from Iran: palaeographic implications: complementary reference*. Chem. Geol., 39, 39-63.

Dewey J.F. and Bird J.M.; 1971: *Origin and emplacement of the ophiolite suite: Appalachian ophiolites in newfoundland*. J. Geophys. Res., 76, 3179-3206.

Dilek Y.; 2003: *Ophiolite concept and its evolution*. In: Dilek Y. and Newcomb S. (eds), Ophiolite concept and the evolution of geological thought, Geological Society of America, Boulder, CO, USA, Special Paper 373, pp. 1-16, doi: 10.1130/0-8137-2373-6.1.

Dilek Y. and Furnes H.; 2011: *Ophiolite genesis and global tectonics: geochemical and tectonic fingerprinting of ancient oceanic lithosphere*. Geol. Soc. Am. Bull., 123, 387-411, doi: 10.1130/B30446.1.

Dilek Y. and Furnes H.; 2014: *Ophiolites and their origins.* Elem., 10, 93-100, doi: 10.2113/gselements.10.2.93.

Fournier D.; 2015: *A cooperative magnetic inversion method with L_p-norm regularization*. Master of Science Thesis in Geophysics, University of British Columbia, Vancouver, Canada, 155 pp., doi: 10.14288/1.0166794.

Fournier D.; 2019: *Advanced potential field data inversion with ℓp-norm regularization.* PH.D. Thesis in Geophysics, University of British Columbia, Vancouver, Canada, 178 pp., doi: 10.14288/1.0380907.

Gandhi S.M. and Sarkar B.C.; 2016: *Geological exploration.* In: Gandhi S.M. and Sarkar B.C., Essentials of Mineral Exploration and Evaluation 1st ed., Elsevier, Amsterdam, The Netherlands, Chapter 7, pp. 159-198, doi: 10.1016/C2015-0-04648-2.

Ghiasi S.M., Hosseini S.H., Afshar A. and Abedi M.; 2023: *A novel magnetic interpretational perspective on Charmaleh iron deposit through improved edge detection techniques and 3D inversion approaches*. Nat. Resour. Res., 32, 147-170.

Ghobadian V., Ghods A. and Rezaeian M.; 2014: *Differential reduction to pole of aeromagnetic data of Iran*. Iran. J. Geophys., 8, 41-55.

Hosseini S.H., Habibian Dehkordi B., Abedi M. and Oskooi B.; 2021: *Implications for a geothermal reservoir at Abgarm, Mahallat, Iran: magnetic and magnetotelluric signatures*. Nat. Resour. Res., 30, 259-272.

Lench G., Mihm A. and Alavi-Tehrani N.; 1977: *Petrography and geology of the ophiolite belt north of Sabzevar/ Khorasan (Iran)*. Neues Jahrb. Mineral. Abh., 131, 156-178.

Li Y. and Oldenburg D.W.; 1996: *3-D inversion of magnetic data*. Geophys., 61, 394-408.

Li Y. and Oldenburg D.W.; 1998: *3-D inversion of gravity data*. Geophys., 63, 109-119.

Li Y. and Oldenburg D.W.; 2003: *Fast inversion of large-scale magnetic data using wavelet transforms and a logarithmic barrier method*. Geophys. J. Int., 152, 251-265.

Michels A., McEnroe S. and Fichler C.; 2018: *Geophysical expression of the Leka Ophiolite, Norway modeled from integrated gravity, magnetic and petrophysical data*. Nor. Geol. Tidsskr., 98, 103-125.

Miller H.G. and Singh V.; 1994: *Potential field tilt - a new concept for location of potential field sources*. J. Appl. Geophys., 32, 213-217.

Moghadam H.S., Corfu F., Chiaradia M., Stern R.J. and Ghorbani G.; 2014: *Sabzevar Ophiolite, NE Iran: progress from embryonic oceanic lithosphere into magmatic arc constrained by new isotopic and geochemical data*. Lithos, 210-211, 224-241, doi: 10.1016/j.lithos.2014.10.004.

Moghaddam M.M., Mirzaei S. and Abedi M.; 2022: *New insights into interpretation of aeromagnetic data for distribution of igneous rocks in central Iran.* Russ. Geol. Geophys., 63, 1061-1077.

Nabighian M.N.; 1972: *The analytic signal of two-dimensional magnetic bodies with polygonal cross-section: its properties and use for automated anomaly interpretation*. Geophys., 37, 507-517.

Nabighian M.N.; 1974: *Additional comments on the analytic signal of two-dimensional magnetic bodies with polygonal cross-section*. Geophys., 39, 85-92.

Noghreyan M.K.; 1982: *Evolution geochimique, mineralogique et structurale d'un edifice ophiolitique singulier: le massif de Sabzevar (partie centrale) NE de l'Iran.* These Doc. d'Etat, Universite de Nancy, Nancy, France, 239 pp.

Nozaem R., Mohajjel M., Rossetti F., Della Seta M., Vignaroli G., Yassaghi A. and Eliassi M.; 2013: *Post-Neogene right-lateral strike-slip tectonics at the north-western edge of the Lut Block (Kuh-e-Sarhangi Fault), central Iran*. Tectonophys., 589, 220-233.

Ohnenstetter M. and Sider H.; 1988: *Contraintes géochimiques apportées par le magmatisme sur le développement du bassin marginal ensialique du Beaujolais au Dévonien*. Bull. Soc. Geol. Fr., 4, 499-510.

Oldenburg D.W. and Li Y.; 2005: *Inversion for applied geophysics: a tutorial.* In: Butler D.K. (ed), Near-surface geophysics, Society of Exploration Geophysicists, Houston, TX, USA, Chapter 5, 89-150, doi: 10.1190/1.9781560801719.ch5.

Omrani H., Moazzen M., Oberhänsli R., Altenberger U. and Lange M.; 2013: *The Sabzevar blueschists of the north-central Iranian micro-continent as remnants of the Neotethys-related oceanic crust subduction*. Int. J. Earth Sci., 102, 1491-1512.

Rossetti F., Nasrabady M., Vignaroli G., Theye T., Gerdes A., Razavi M.H. and Vaziri H.M.; 2010: *Early Cretaceous migmatitic mafic granulites from the Sabzevar range (NE Iran): implications for the closure of the Mesozoic peri-Tethyan oceans in central Iran*. Terra Nova, 22, 26-34.

Saleh R.; 2006: *Reprocessing of aeromagnetic map of Iran.* Master of Science Thesis in Geophysics, Institute for Advanced Studies in Basic Sciences, Zanjan, Iran, 169 pp., in Persian with English abstract.

Şengör A.M.C.; 1990: *Plate tectonics and orogenic research after 25 years: a Tethyan perspective*. Earth Sci. Rev., 27, 1-201.

Shojaat B., Hassanipak A.A., Mobasher K. and Ghazi A.M.; 2003: *Petrology, geochemistry and tectonics of the Sabzevar ophiolite, north central Iran*. J. Asian Earth Sci., 21, 1053-1067.

Takin M.; 1972: *Iranian geology and continental drift in the Middle East*. Nature, 235, 147-150.

Verduzco B., Fairhead J.D., Green C.M. and MacKenzie C.; 2004: *New insights into magnetic derivatives for structural mapping*. The Leading Edge, 23, 116-119.

Yousefi E. and Friedberg J.L.; 1977: *Aeromagnetic map of Iran quadrangle.* Geological Survey of Iran, Tehran, Iran, F5.

Corresponding author: Maysam Abedi
School of Mining Engineering, University of Tehran
Amirabad, 98 Tehran, Iran
Phone: +98 21 61114563; e-mail: maysamabedi@ut.ac.ir